



# Reflection by and transmission through an ENZ interface

ZHANGJIN XU AND HENK F. ARNOLDUS\*

*Department of Physics and Astronomy, Mississippi State University, P.O. Box 5167, Mississippi State, Mississippi 39762, USA*

\**hfa1@msstate.edu*

**Abstract:** We have studied the reflection and transmission of traveling and evanescent plane waves, incident upon an ENZ material. The Fresnel reflection and transmission coefficients were obtained in the ENZ limit. For a  $p$  polarized incident wave, the transmission coefficient vanishes, except very close to normal incidence. The reflection coefficient is -1 for both traveling and evanescent waves. It is shown, however, that there is a finite electric field in the ENZ material, even though the transmission coefficient is zero. This field is either linearly polarized or circularly polarized. The magnetic field in the medium for  $p$  polarized illumination is zero, and therefore there can be no energy flow through the material. For  $s$  polarization, the magnetic field in the medium is circularly polarized, and energy can flow through the material, parallel to the interface.

© 2019 Optical Society of America under the terms of the [OSA Open Access Publishing Agreement](#)

## 1. Introduction

The electromagnetic properties of a linear isotropic homogeneous material are determined by the relative permittivity  $\varepsilon$  and the relative permeability  $\mu$ . We shall suppress the common subscript  $r$ . These parameters of the (non-gain) medium are in general complex with a non-negative imaginary part. They depend on the angular frequency  $\omega$  of the radiation under consideration. We shall assume monochromatic irradiation, so that this frequency dependence becomes irrelevant. The index of refraction  $n$  is a solution of

$$n^2 = \varepsilon\mu, \quad \text{Im } n \geq 0. \quad (1)$$

This leaves an ambiguity when  $\varepsilon$  and  $\mu$  are both real and have the same sign. By including small positive imaginary parts in the parameters, we then find that  $n$  should be taken as having the same sign as  $\varepsilon$  and  $\mu$  [1]. For natural occurring dielectrics,  $\varepsilon$  and  $\mu$  are positive, and so is  $n$ . Metamaterials are artificial media that can have, in principle, any values of  $\varepsilon$  and  $\mu$ , with the restriction that their imaginary parts are non-negative. Ingenious sub-wavelength structures have been proposed theoretically and tested experimentally in order to construct materials with parameters  $\varepsilon$  and  $\mu$  that do not occur in nature.

In the past decades, a great deal of effort has been devoted to the development of so-called double negative metamaterials. For these materials  $\varepsilon$  and  $\mu$  are both negative (with inevitable small positive imaginary parts), and therefore the index of refraction is approximately real and negative. These negative index of refraction materials (NIM's) have been predicted to have peculiar properties by Vesalago [2]. A plane wave that refracts into the medium at an interface appears at the opposite side of the surface normal as compared to refraction into a regular dielectric with positive  $n$ . Later, Pendry [3] showed that incident evanescent waves could possibly be amplified by a slab of NIM, leaving a possible path to the construction of a superlens that can resolve images below the diffraction limit. Some controversies regarding the Fresnel reflection and transmission coefficients for such a layer were resolved in [4].

The Green's function for the emission of radiation by a localized source, embedded in a medium with index of refraction  $n$ , is given by

$$g(r) = \exp(ink_0 r)/r, \quad (2)$$

where  $k_0 = \omega/c$  is the wave number in free space. Here,  $r$  is the distance between the field point and a point inside the source. For a point source, like a dipole, located at the origin of coordinates, this is just the spherical coordinate  $r$  of the field point. For a NIM with the real part of  $n$  negative and the imaginary part of  $n$  positive, this is an incoming spherical wave which damps out in amplitude in the outgoing direction. Obviously, the energy propagates outward, but the spherical wave carrying the energy travels inward. Similarly, the energy in a traveling plane wave propagates against the wave vector.

More recently, materials with epsilon-near-zero (ENZ) have attracted a great deal of attention. We shall assume that  $\mu = 1$ , so that  $n = \sqrt{\epsilon}$  is the correct solution of Eq. (1). We then have  $n \approx 0$ , and we see from Eq. (2) that the Green's function for wave propagation in an ENZ material becomes  $g(r) \approx 1/r$ . The time dependence for a monochromatic field is taken as  $\exp(-i\omega t)$ . The expected spherical wave becomes  $\exp(-i\omega t)/r$ . The field oscillates with angular frequency  $\omega$ , but the spatial oscillations have disappeared. This phenomenon is referred to as 'static optics'. The field still oscillates with time  $t$ , but the spatial part becomes  $g(r) \approx 1/r$ , which is the Green's function of electrostatics. One may then wonder whether any energy transport is possible through such a material.

ENZ materials exist in nature. Most notably, if  $\omega$  of the source is close to the plasma frequency of a metal, the  $\epsilon$  of the metal is close to zero. Below the plasma frequency the metal is opaque and above the plasma frequency it is transparent. However, these plasma frequencies are in the UV (wavelength  $\sim 130$  nm for gold). Metamaterial ENZ media have been demonstrated in the microwave region [5–7], for terahertz radiation [8,9] and for the visible range of the spectrum [10,11], and have been studied theoretically [12–18]. An interesting application of ENZ media is the possibility of squeezing, funneling or tunneling electromagnetic radiation through narrow channels or bends [19–24]. Also waveform shaping and angular filtering has been proposed [25–28], and levitation of small particles near the surface of an ENZ interface has been predicted [29]. Other applications include perfect optical absorbers [30,31] and enhancement of the magneto-optical effect [32].

The electric and magnetic fields emitted by a localized source can be represented in terms of the scalar Green's function of Eq. (2) [33,34]. When this function is represented by an angular spectrum [35], the fields become superpositions (integrals) over plane waves. These waves are either traveling or evanescent, with respect to the surface of the material, and they are either  $s$  or  $p$  polarized. The reflected and transmitted plane waves can then be constructed with the help of appropriate Fresnel coefficients, and the reflected electric and magnetic fields then follow by superposition. This approach has proven to be very successful for the study of the radiation pattern of an electric dipole near an interface [36], and for the computation of the field lines of energy flow in the near field [37,38]. In order to tackle this problem for an ENZ medium, it is imperative to study the solutions for plane waves first, and in particular include the evanescent incident plane waves.

## 2. Traveling and evanescent waves

We shall assume a harmonic time dependence with angular frequency  $\omega$ . Then the electric field is represented as

$$\mathbf{E}(\mathbf{r}, t) = \text{Re}[\mathbf{E}(\mathbf{r}) \exp(-i\omega t)], \quad (3)$$

with  $\mathbf{E}(\mathbf{r})$  the complex amplitude, and the magnetic field  $\mathbf{B}(\mathbf{r}, t)$  is written similarly. The incident field is a plane wave with wave vector  $\mathbf{k}_i$ , as shown in Fig. 1. It travels in vacuum towards an interface with a material having permittivity  $\epsilon$ . We shall assume that the parallel component  $\mathbf{k}_{\parallel}$  of this wave vector is real, and given. A plane wave of an angular spectrum representation of a radiation field has this  $\mathbf{k}_{\parallel}$  as the free variable, and in the superposition this becomes the summation (integration) variable. Since the wave travels in vacuum, it has to hold that

$\mathbf{k}_i \cdot \mathbf{k}_i = (\omega/c)^2$ , and this is  $\mathbf{k}_i \cdot \mathbf{k}_i = k_0^2$ . When we set  $\mathbf{k}_i = \mathbf{k}_{||} + k_{i,z}\mathbf{e}_z$  this gives  $k_{||}^2 + k_{i,z}^2 = k_0^2$ , and this is an equation for  $k_{i,z}$ , since  $k_{||} = |\mathbf{k}_{||}|$  and  $k_0$  are given. We now introduce the parameter

$$\alpha = k_{||}/k_0, \tag{4}$$

and we set

$$v_1 = \sqrt{1 - \alpha^2}. \tag{5}$$

Then the two solutions for  $k_{i,z}$  are  $\pm k_0 v_1$ . Parameter  $\alpha$  is the dimensionless representation of the magnitude of  $\mathbf{k}_{||}$ , and this is considered to be the free variable. For  $0 \leq \alpha < 1$  we see that  $v_1$  is real and positive. Therefore  $\mathbf{k}_i$  is a real vector, and we have a traveling incident wave. We then take the solution  $k_{i,z} = v_1 k_0$  for which the wave travels in the positive  $z$  direction. This wave is represented by arrow  $\mathbf{k}_i$  in Fig. 1. It is easy to see that  $\alpha = \sin \theta_i$ , with  $\theta_i$  the angle of incidence. On the other hand, when  $\alpha > 1$  we find that  $v_1$  is positive imaginary. We take again the solution  $k_{i,z} = v_1 k_0$ , so that the wave decays exponentially in the positive  $z$  direction. The incident wave is now evanescent, and is indicated schematically by the parallel lines in Fig. 1. Such waves still travel along the surface with wave vector  $\mathbf{k}_{||}$ . The integration variable in an angular spectrum, after integration over the direction of  $\mathbf{k}_{||}$  is the parameter  $\alpha$ , with  $0 \leq \alpha < \infty$ .

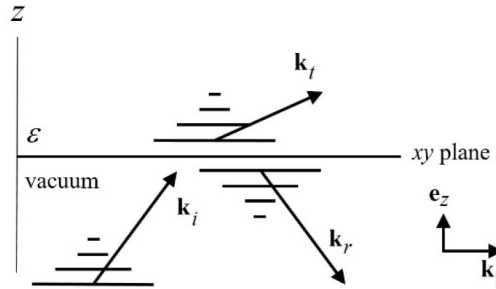


**Fig. 1.** Illustration of a travelling or an evanescent plane wave reflecting off and transmitting into a dielectric. We take the positive  $z$  direction as up.

The wave vectors  $\mathbf{k}_r$  and  $\mathbf{k}_t$  of the reflected wave and the transmitted wave, respectively, must have the same parallel component  $\mathbf{k}_{||}$  as the wave vector  $\mathbf{k}_i$  of the incident wave. The wave vector of the incident wave is

$$\mathbf{k}_i = \mathbf{k}_{||} + k_0 v_1 \mathbf{e}_z, \tag{6}$$

and since the reflected wave is also in vacuum, we must have

$$\mathbf{k}_r = \mathbf{k}_{||} - k_0 v_1 \mathbf{e}_z. \tag{7}$$

For  $0 \leq \alpha < 1$  this wave is traveling and for  $\alpha > 1$  the reflected wave is evanescent. The transmitted wave is in the medium with permittivity  $\epsilon$ , so we must have  $k_{||}^2 + k_{t,z}^2 = \epsilon k_0^2$ . The causal solution is

$$\mathbf{k}_t = \mathbf{k}_{||} + k_0 v_2 \mathbf{e}_z, \tag{8}$$

with

$$v_2 = \sqrt{n^2 - \alpha^2}, \tag{9}$$

and  $n = \sqrt{\epsilon}$ .

Let us now consider what kind of wave the  $t$  wave is. Let us assume for a moment that  $\epsilon$  is positive, like in good approximation for most dielectrics. Then also  $n$  is positive. If  $\alpha < n$ , then  $v_2$  is real, and the  $t$  wave is traveling. If  $\alpha > n$ , then  $v_2$  is imaginary, and the  $t$  wave is evanescent. If

the incident wave is traveling, then  $\alpha$  is in the range  $0 \leq \alpha < 1$ , and  $\alpha = \sin \theta_i$  with  $\theta_i$  the angle of incidence. If  $n > 1$ , then  $\alpha < n$  for all  $\alpha$ , and thus the  $t$  wave is traveling. If  $n < 1$ , the  $t$  wave is traveling for  $0 \leq \alpha < n$  and evanescent for  $n < \alpha < 1$ . Borderline is  $\alpha = n$ , and this is  $\sin \theta_i = n$ . This is the familiar critical angle. If the incident wave is evanescent, we have  $\alpha > 1$ . If  $n < 1$ , the  $t$  wave is evanescent for all  $\alpha$ . If  $n > 1$ , the  $t$  wave is evanescent for  $\alpha > n$  and traveling for  $1 < \alpha < n$ . In the latter case we have the unusual situation that an evanescent incident wave is converted into a traveling wave upon transmission through the interface. For a metallic medium we have  $\varepsilon < 0$ , and  $n$  is positive imaginary. The  $t$  wave is evanescent for all  $\alpha$ . When  $\varepsilon$  is complex, with a positive imaginary part, then so is  $n$ . In addition, the real part of  $n$  is positive. Then the  $t$  wave is partially traveling and partially evanescent in the  $z$  direction.

### 3. Polarization vectors

When the incident wave is  $s$  polarized (TE), then so are the reflected and transmitted waves. The same holds for  $p$  polarization (TM). The unit vector in the  $\mathbf{k}_{||}$  direction is

$$\hat{\mathbf{k}}_{||} = \frac{1}{\alpha k_0} \mathbf{k}_{||}. \quad (10)$$

The unit vector for  $s$  polarization is taken to be

$$\mathbf{e}_s = \mathbf{e}_z \times \hat{\mathbf{k}}_{||}, \quad (11)$$

which is perpendicular to the plane of the page in Fig. 1, and into the page. The unit vectors for  $p$  polarization are defined as

$$\mathbf{e}_{p,\ell} = \frac{1}{k_0} \mathbf{k}_\ell \times \mathbf{e}_s, \quad \ell = i, r, \quad (12)$$

$$\mathbf{e}_{p,t} = \frac{1}{nk_0} \mathbf{k}_t \times \mathbf{e}_s. \quad (13)$$

With the wave vectors given by Eqs. (6–8), we find explicitly

$$\mathbf{e}_{p,i} = \alpha \mathbf{e}_z - v_1 \hat{\mathbf{k}}_{||}, \quad (14)$$

$$\mathbf{e}_{p,r} = \alpha \mathbf{e}_z + v_1 \hat{\mathbf{k}}_{||}, \quad (15)$$

$$\mathbf{e}_{p,t} = \frac{1}{n} (\alpha \mathbf{e}_z - v_2 \hat{\mathbf{k}}_{||}), \quad (16)$$

and these lie in the plane of the paper in Fig. 1, although they may be complex-valued. The normalization is chosen such that

$$\mathbf{e}_{\sigma,\ell} \cdot \mathbf{e}_{\sigma,\ell} = 1, \quad \sigma = s, p, \quad \ell = i, r, t. \quad (17)$$

Furthermore, the polarization vectors are orthogonal to the corresponding wave vectors:

$$\mathbf{e}_{\sigma,\ell} \cdot \mathbf{k}_\ell = 0, \quad \sigma = s, p, \quad \ell = i, r, t, \quad (18)$$

and obviously every  $s$  polarization vector is orthogonal to the corresponding  $p$  polarization vector.

#### 4. Fields and Fresnel coefficients

The incident plane wave has wave vector  $\mathbf{k}_i$  and amplitude  $E_o$ , which may be complex. The expressions for the reflected and transmitted waves are plane waves with the corresponding wave vectors and polarization vectors. The amplitudes are  $E_o$  times the appropriate Fresnel coefficients. We find for  $s$  polarization

$$\mathbf{E}(\mathbf{r})_1 = E_o \exp(i\mathbf{k}_{||} \cdot \mathbf{r}) \mathbf{e}_s [\exp(iv_1 \bar{z}) + R_s \exp(-iv_1 \bar{z})], \quad (19)$$

$$\mathbf{B}(\mathbf{r})_1 = (E_o/c) \exp(i\mathbf{k}_{||} \cdot \mathbf{r}) [\mathbf{e}_{p,t} \exp(iv_1 \bar{z}) + R_s \mathbf{e}_{p,r} \exp(-iv_1 \bar{z})], \quad (20)$$

$$\mathbf{E}(\mathbf{r})_2 = E_o \exp(i\mathbf{k}_{||} \cdot \mathbf{r}) T_s \mathbf{e}_s \exp(iv_2 \bar{z}), \quad (21)$$

$$\mathbf{B}(\mathbf{r})_2 = n(E_o/c) \exp(i\mathbf{k}_{||} \cdot \mathbf{r}) T_s \mathbf{e}_{p,t} \exp(iv_2 \bar{z}), \quad (22)$$

where the subscripts 1 and 2 refer to the vacuum and the medium, respectively. We have set  $\bar{z} = k_o z$  for the dimensionless  $z$  coordinate of the field point. Similarly, for  $p$  polarization we have

$$\mathbf{E}(\mathbf{r})_1 = E_o \exp(i\mathbf{k}_{||} \cdot \mathbf{r}) [\mathbf{e}_{p,i} \exp(iv_1 \bar{z}) + R_p \mathbf{e}_{p,r} \exp(-iv_1 \bar{z})], \quad (23)$$

$$\mathbf{B}(\mathbf{r})_1 = -(E_o/c) \exp(i\mathbf{k}_{||} \cdot \mathbf{r}) \mathbf{e}_s [\exp(iv_1 \bar{z}) + R_p \exp(-iv_1 \bar{z})], \quad (24)$$

$$\mathbf{E}(\mathbf{r})_2 = E_o \exp(i\mathbf{k}_{||} \cdot \mathbf{r}) T_p \mathbf{e}_{p,t} \exp(iv_2 \bar{z}), \quad (25)$$

$$\mathbf{B}(\mathbf{r})_2 = -n(E_o/c) \exp(i\mathbf{k}_{||} \cdot \mathbf{r}) T_p \mathbf{e}_s \exp(iv_2 \bar{z}). \quad (26)$$

The magnetic field in the medium is proportional to  $n$  for both polarizations. This may seem to lead to the conclusion that these fields vanish in the ENZ limit. We shall show below that this is not necessarily the case. The expressions for the Fresnel coefficients follow by applying the usual boundary conditions at the interface. This yields

$$R_s(\alpha) = \frac{v_1 - v_2}{v_1 + v_2}, \quad (27)$$

$$T_s(\alpha) = \frac{2v_1}{v_1 + v_2}, \quad (28)$$

$$R_p(\alpha) = \frac{\varepsilon v_1 - v_2}{\varepsilon v_1 + v_2}, \quad (29)$$

$$T_p(\alpha) = \frac{2nv_1}{\varepsilon v_1 + v_2}. \quad (30)$$

#### 5. ENZ limit of the Fresnel coefficients

For an ENZ medium we have  $\varepsilon \rightarrow 0$  and  $n \rightarrow 0$ . This gives  $v_2 \rightarrow i\alpha$  and  $v_1$  remains as is, Eq. (5). In Eqs. (27–29) we can immediately take this limit, with result

$$R_s(\alpha)^{ENZ} = (v_1 - i\alpha)^2, \quad (31)$$

$$T_s(\alpha)^{ENZ} = 2v_1(v_1 - i\alpha), \quad (32)$$

$$R_p(\alpha)^{ENZ} = -1. \quad (33)$$

The expression for  $T_p(\alpha)$  seems to go to zero for  $n \rightarrow 0$ . However, if  $\alpha = 0$  (normal incidence of a traveling wave), then both numerator and denominator go to zero. Then  $v_1 = 1$  and  $v_2 = n$ . With  $\varepsilon = n^2$  we then get  $T_p(0)^{ENZ} = 2$ . So,

$$T_p(\alpha)^{ENZ} = \begin{cases} 0 & , \quad \alpha \neq 0 \\ 2 & , \quad \alpha = 0 \end{cases}. \quad (34)$$

Let us now consider some of the properties of the Fresnel coefficients. In the following graphs, we plot the Fresnel coefficients as a function of  $\alpha$ . The solid lines are the ENZ limits and the

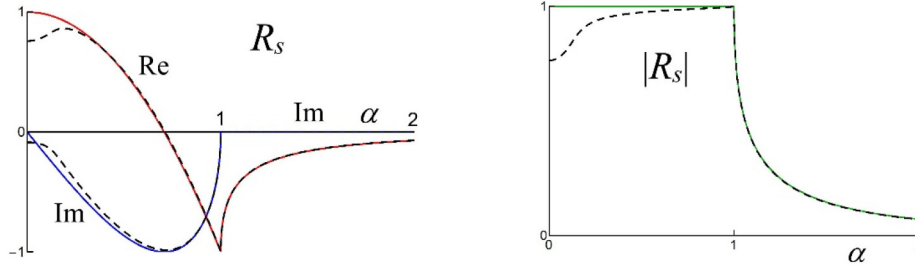


**Fig. 2.** The figure on the left shows the real and imaginary parts of the reflection coefficient for  $s$  waves. The dashed lines are for the small value of  $\epsilon = 0.015 \times (1 + i)$ , and the solid lines are the ENZ limits, with the real part red and the imaginary part blue. The figure on the right shows the ENZ limit of the absolute value of  $R_s$  (green curve), with the dashed line the result for the same small  $\epsilon$  as in the figure on the left.

dashed lines are the values for a hypothetical medium with  $\epsilon = 0.015 \times (1 + i)$ . Figure 2 shows the real and imaginary parts of  $R_s(\alpha)$ , and  $|R_s(\alpha)|$ . For evanescent waves, the imaginary part in the ENZ limit is identically zero. We see that

$$|R_s(\alpha)^{ENZ}| = 1 \quad , \quad 0 \leq \alpha < 1, \tag{35}$$

as can also be shown explicitly with Eq. (31). This means that a traveling wave undergoes a phase shift upon reflection, but the amplitude of the reflected wave is the same as the amplitude of the incident wave. For evanescent waves, however, the amplitude of the reflected wave is smaller than the amplitude of the incident wave, and the amplitude ratio decreases with  $\alpha$ . Figure 3 shows the real and imaginary parts of  $T_s$ , and  $|T_s|$ . Again, the imaginary part is identically zero for evanescent waves. The real part, however, grows with  $\alpha$ . For normal incidence we have  $T_s(0)^{ENZ} = 2$ , and for grazing incidence ( $\alpha = 1$ ) we have  $T_s(1)^{ENZ} = 0$ . For  $0 \leq \alpha < 1$  the incident wave is traveling, and  $v_1$  is real, with  $0 < v_1 \leq 1$ . Since  $v_1^2 = 1 - \alpha^2$  we have  $|v_1 + i\alpha| = 1$ . Therefore,  $v_1 + i\alpha$  is on the unit circle in the complex plane. For the phase angle  $\theta$  we have  $\sin \theta = \alpha$ . For a traveling wave,  $\alpha$  is the sine of the angle of incidence, so we conclude that this phase angle is  $\theta_i$ . We then have

$$v_1 + i\alpha = \exp(i\theta_i). \tag{36}$$

The Fresnel reflection and transmission coefficients from Eqs. (31) and (32) become

$$R_s(\alpha)^{ENZ} = \exp(-2i\theta_i), \tag{37}$$

$$T_s(\alpha)^{ENZ} = 2v_1 \exp(-i\theta_i). \tag{38}$$

Relation (35) now follows immediately from Eq. (37).

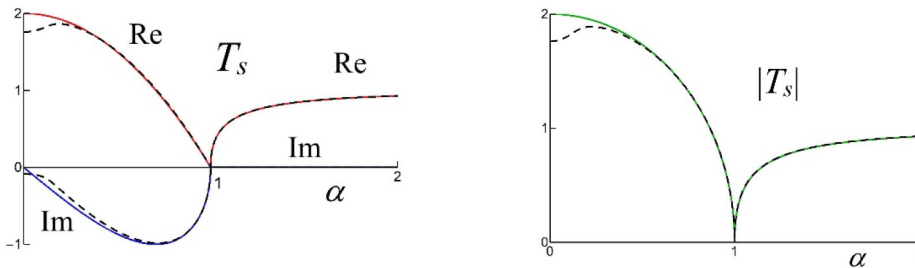


**Fig. 3.** Shown are the real and imaginary parts of  $T_s$ , and the absolute value of  $T_s$ , for small  $\epsilon$  (dashed curves). The solid curves are the ENZ limits.

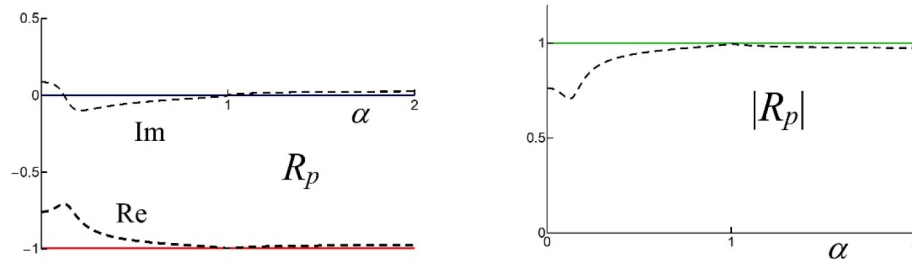


**Fig. 4.** Shown are the real and imaginary parts of  $R_p$ , and the absolute value of  $R_p$ , for small  $\varepsilon$  (dashed curves). The solid curves are the ENZ limits.

Let us now consider  $p$  waves. We see from Eq. (33) that the reflection coefficient is  $-1$  for all  $\alpha$ . Any  $p$  wave reflects back with only a phase shift, and this phase shift is the same for all  $\alpha$ . This behavior is illustrated in Fig. 4. The transmission coefficient vanishes for all  $\alpha$ , except  $\alpha = 0$ , as shown in Fig. 5. It seems that no radiation penetrates the material for  $\alpha \neq 0$ . This would be the same as for a perfect conductor (mirror). We shall show below that for an ENZ material this conclusion is incorrect. The dashed curves for the small value  $\varepsilon = 0.015 \times (1 + i)$  in Fig. 5 are not close to the ENZ limit for traveling waves, which is zero for all  $\alpha$ , except  $\alpha = 0$ .  $T_p(\alpha)^{ENZ}$  in Eq. (34) has a discontinuity at normal incidence. Such a point singularity is obviously unphysical. The interpretation of this phenomenon can be inferred from Fig. 5. For  $\varepsilon \rightarrow 0$ , the imaginary part vanishes, and the real part has a sharp peak near  $\alpha = 0$ , with a height of 2. From Eq. (9) for  $v_2$  we see that in the ENZ limit and  $\alpha \rightarrow 0$  we have  $v_2 \rightarrow 0$ . However, the limits  $n \rightarrow 0$  and  $\alpha \rightarrow 0$  do not commute. For  $n = 0$  and  $\alpha \rightarrow 0$  we have  $T_p(\alpha) \rightarrow 0$ , but for  $\alpha = 0$  and  $n \rightarrow 0$  we have  $T_p(0) \rightarrow 2$ . Physically, neither  $n$  nor  $\alpha$  can be exactly zero. Whether  $T_p(\alpha) \rightarrow 0$  for  $n = 0$  or  $T_p(0) \rightarrow 2$  depends on which one is smaller:  $|n|$  or  $\alpha$ . As mentioned in Sec. 2, the critical angle (of incidence) is at  $n = \alpha = \sin \theta_i$  (for  $n$  real). For any  $n$ , there will always be a small range  $0 \leq \alpha < |n|$  for which  $T_p(\alpha) \approx 2$ , and the transmitted wave is (partially) traveling. Outside this range, the transmitted wave is mainly evanescent, and  $T_p(\alpha) \approx 0$ . For  $\varepsilon = 0.015 \times (1 + i)$  we have  $n = 0.13 + 0.056 \times i$  and  $|n| = 0.15$  as the upper limit on  $\alpha$ . This corresponds to an angle of incidence of about  $8^\circ$ .

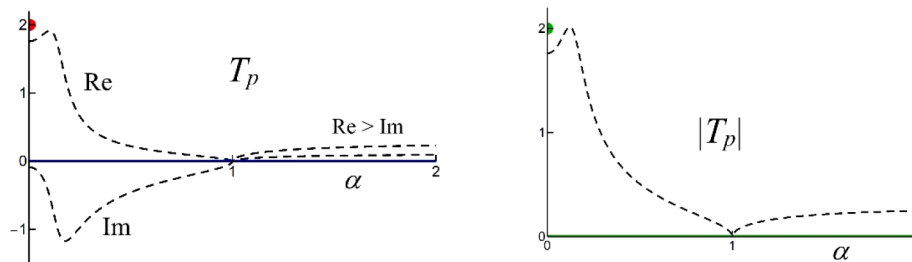


**Fig. 5.** Shown are the real and imaginary parts of  $T_p$ , and the absolute value of  $T_p$ , for small  $\varepsilon$  (dashed curves). The solid curves are the ENZ limits. For evanescent waves, the values of the real and imaginary parts of  $T_p$  are close to their ENZ limit of zero, with the real part larger than the imaginary part. For traveling waves, the convergence to the ENZ limit is much slower. The dot represents  $T_p(0)^{ENZ} = 2$ . For  $\alpha \neq 0$  we have  $T_p = 0$ , which is the green line in the figure on the right. In the figure on the left, the red and blue lines are on top of each other, making it look purple.

Finally, we mention that for  $\alpha \approx 0$  the distinction between  $s$  and  $p$  waves should disappear. We see from Figs. 2 and 4 that  $R_s \approx 1$  and  $R_p \approx -1$ . The difference in sign is due to the phase conventions for the polarization vectors. From Figs. 3 and 5 we see that  $T_s \approx 2$  and  $T_p \approx 2$ .

### 6. ENZ limit of the fields

We now consider the fields from Eqs. (19–26) in the ENZ limit. Nothing simplifies for the incident and reflected waves, except that  $R_p \rightarrow -1$  in Eqs. (23) and (24), and  $R_s$  in Eqs. (19) and (20) can be replaced by the right-hand side of Eq. (31). In the medium,  $v_2 \rightarrow i\alpha$ , and so  $\exp(iv_2\bar{z}) \rightarrow \exp(-\alpha\bar{z})$ . All fields in the ENZ medium are evanescent, with  $\alpha = 0$  borderline.

Let us first look at the  $s$  waves. In Eq. (22) we have the product  $n\mathbf{e}_{p,t}$ . From Eq. (16) we see that  $\mathbf{e}_{p,t} \propto 1/n$ , so the factor  $n$  cancels. We then get  $n\mathbf{e}_{p,t} = \alpha\mathbf{e}_z - v_2\hat{\mathbf{k}}_{||}$ , and with  $v_2 \rightarrow i\alpha$  this yields  $n\mathbf{e}_{p,t} \rightarrow \alpha\boldsymbol{\eta}$ , with

$$\boldsymbol{\eta} = \mathbf{e}_z - i\hat{\mathbf{k}}_{||}. \tag{39}$$

The  $t$  wave for  $s$  polarization becomes

$$\mathbf{E}(\mathbf{r})_2 = 2E_0v_1(v_1 - i\alpha)\exp(i\mathbf{k}_{||} \cdot \mathbf{r})\mathbf{e}_s\exp(-\alpha\bar{z}), \tag{40}$$

$$\mathbf{B}(\mathbf{r})_2 = 2\alpha(E_0/c)v_1(v_1 - i\alpha)\exp(i\mathbf{k}_{||} \cdot \mathbf{r})\boldsymbol{\eta}\exp(-\alpha\bar{z}), \tag{41}$$

where we have replaced  $T_s$  by the right-hand side of Eq. (32). The electric field is still  $s$  polarized, but the polarization vector  $\mathbf{e}_{p,t}$  of the magnetic field has become  $\boldsymbol{\eta}$ . In order to see the significance of this, we note that the right-hand side of Eq. (38) is the complex amplitude of the magnetic field

$$\mathbf{B}_2(\mathbf{r}, t) = \text{Re}[\mathbf{B}_2(\mathbf{r})\exp(-i\omega t)]. \tag{42}$$

For a fixed point  $\mathbf{r}$  in the ENZ medium we set temporarily

$$2\alpha(E_0/c)v_1(v_1 - i\alpha)\exp(i\mathbf{k}_{||} \cdot \mathbf{r})\exp(-\alpha\bar{z}) = A\exp(i\phi) \quad , \quad A > 0 \quad , \quad \phi \text{ real}. \tag{43}$$

Then

$$\mathbf{B}_2(\mathbf{r}, t) = A\text{Re}\{\boldsymbol{\eta}\exp[-i(\omega t - \phi)]\}, \tag{44}$$

and this is

$$\mathbf{B}_2(\mathbf{r}, t) = A[\mathbf{e}_z \cos(\omega t - \phi) - \hat{\mathbf{k}}_{||} \sin(\omega t - \phi)]. \tag{45}$$

Vector  $\mathbf{B}_2(\mathbf{r}, t)$  has magnitude  $A$ , and as a function of time it rotates in the plane of incidence in the direction from  $\hat{\mathbf{k}}_{||}$  to  $\mathbf{e}_z$ . This is counterclockwise in Fig. 1. The magnetic field in the medium is circularly polarized, although not in the usual sense. Now let us set

$$2\alpha(E_0/c)v_1(v_1 - i\alpha) = C\exp(i\psi) \quad , \quad C > 0 \quad , \quad \psi \text{ real}, \tag{46}$$

and take the  $y$  axis along  $\hat{\mathbf{k}}_{||}$ . Then we have

$$\mathbf{B}_2(\mathbf{r}, t) = C\exp(-\alpha\bar{z})\text{Re}\{(\mathbf{e}_z - i\mathbf{e}_y)\exp[i(k_{||}y - \omega t + \psi)]\}. \tag{47}$$

We first notice that the field has no  $x$  dependence, so it is constant into the direction perpendicular to the page in Fig. 1. The magnetic field is the same in every plane parallel to the incident plane. The  $z$  dependence comes in as  $\exp(-\alpha\bar{z})$ , so the amplitude decays exponentially into the direction perpendicular to the interface (up in Fig. 1). The  $y$  and  $t$  dependence enters as

$\exp[i(k_{||}y - \omega t + \psi)]$ . This represents a traveling wave in the  $y$  direction (to the right in Fig. 1), with phase velocity

$$v_{\text{ph}} = \frac{\omega}{k_{||}} = \frac{c}{\alpha}, \quad (48)$$

and wavelength  $\lambda = 2\pi/k_{||}$ . The dimensionless wavelength is  $\bar{\lambda} = k_o\lambda$ , so

$$\bar{\lambda} = \frac{2\pi}{\alpha}. \quad (49)$$

In these units, the free space wavelength is  $\bar{\lambda} = 2\pi$ . If the incident wave is traveling, we have  $0 < \alpha < 1$ , and the phase velocity along the surface is greater than the speed of light. If the incident wave is evanescent, we have  $\alpha > 1$ , and the phase velocity is less than the speed of light. The wavelength is greater than or less than the free space wavelength, respectively. Figure 6 shows field lines of the magnetic field in the plane of incidence for a fixed  $t$ , and  $\alpha = 0.5$ . In each plane parallel to this plane the picture is the same. As a function of time, the field line pattern moves to the right with  $v_{\text{ph}} = 2c$ . The picture is periodic in the horizontal direction with wavelength  $\bar{\lambda} = 4\pi$ . At the vacuum side, the pattern is due to interference between the incident and the reflected wave. The field lines form closed loops with singularities at the centers. Field lines that cross the interface stretch into the medium, and return to the interface to complete the loop in the vacuum side. The magnitude of the magnetic field in the medium decreases exponentially in the upward direction, but this cannot be seen in a field line picture (field lines are determined by the direction of a vector field, but not by its magnitude). The electric field is  $s$  polarized, so its field lines are straight lines, perpendicular to the plane of the page in Fig. 6.

For  $p$  waves we get the factor  $T_p \mathbf{e}_{p,t}$  in Eq. (25). From Eqs. (16) and (30) we see that again a factor of  $n$  cancels. We therefore have two cases, just as for  $T_p$  in Eq. (34). We now find

$$\mathbf{E}(\mathbf{r})_2 = -2E_o \times \begin{cases} \hat{\mathbf{k}}_{||} & , \quad 0 \leq \alpha < |n| \\ i v_1 \boldsymbol{\eta} \exp(i\mathbf{k}_{||} \cdot \mathbf{r}) \exp(-\alpha \bar{z}) & , \quad \alpha > |n| \end{cases}, \quad (50)$$

$$\mathbf{B}(\mathbf{r})_2 = 0. \quad (51)$$

The magnetic field vanished for all  $\alpha$ . Here we have the remarkable situation that even though the transmission coefficient is zero for  $\alpha > |n|$ , there is still a finite electric field in the material. For  $\alpha > |n|$ , the electric field is circular polarized, and for  $0 \leq \alpha < |n|$  this field is linearly polarized. For  $\alpha \rightarrow 0$  the distinction between  $s$  and  $p$  waves should disappear. Comparison with Eqs. (40) and (41) shows that this is indeed the case, provided that for  $p$  waves we take the limit as  $0 \leq \alpha < |n|$  in Eq. (50). Experimentally, the value of  $n$  is fixed for a given material, and it can never be exactly equal to zero. However,  $\alpha = \sin \theta_i$ , and the angle of incidence can be varied from large values to as good as zero. In the neighborhood of  $\sin \theta_i = |n|$ , the polarization of the electric field changes abruptly from circular to linear, and the field becomes identical to the field for  $s$  waves in this limit.

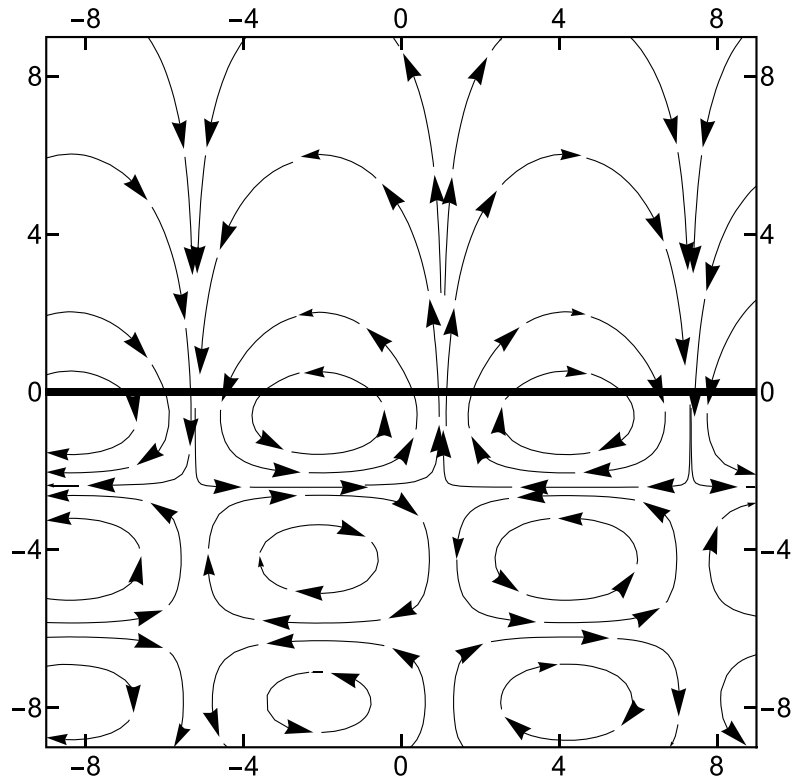


**Fig. 6.** Shown are the field lines of the magnetic field in the plane of incidence, for  $s$  polarization. Here,  $2\pi$  correspond to an optical wavelength in free space. The fat line in the middle is the interface, and the ENZ medium is above it.

## 7. Energy flow

We now return to the question whether or not energy will flow through the ENZ medium. To this end, we consider the time averaged Poynting vector

$$\mathbf{S}(\mathbf{r}) = \frac{1}{2\mu_0} \text{Re}[\mathbf{E}(\mathbf{r}) \times \mathbf{B}(\mathbf{r})^*], \quad (52)$$

containing the complex amplitudes of the electric and magnetic fields. We spilt off a factor

$$\mathbf{S}(\mathbf{r}) = S_0 \mathbf{S}'(\mathbf{r}), \quad (53)$$

with

$$S_0 = \frac{|E_0|^2}{2\mu_0 c}. \quad (54)$$

In this way,  $\mathbf{S}'(\mathbf{r})$  is dimensionless, and  $S_0$  is an overall measure for the field strength. It is advantageous to consider traveling and evanescent incident waves separately.

### 7.1. Traveling incident wave

For  $0 \leq \alpha < 1$  the incident wave is traveling, and parameter  $\nu_1$  from Eq. (5) is real and positive. In the complex conjugate of  $\mathbf{B}(\mathbf{r})$  we can then set  $\nu_1^* = \nu_1$ . For the reflection and transmission

coefficients in the ENZ limit we use Eqs. (37) and (38). We then obtain for  $s$  waves

$$\mathbf{S}(\mathbf{r})'_1 = 4\alpha\hat{\mathbf{k}}_{||}\cos^2(v_1\bar{z} + \theta_i), \quad (55)$$

$$\mathbf{S}(\mathbf{r})'_2 = 4\alpha\hat{\mathbf{k}}_{||}(1 - \alpha^2)\exp(-2\alpha\bar{z}). \quad (56)$$

In the ENZ material, energy flows along the interface in the  $\hat{\mathbf{k}}_{||}$  direction, and the magnitude of the energy flow vector decreases exponentially away from the interface. At the vacuum side, energy also flows in the  $\hat{\mathbf{k}}_{||}$  direction with an oscillating  $z$  dependence. At the interface we have  $\bar{z} = 0$ , and with  $\cos^2\theta_i = 1 - \alpha^2$  we see that the Poynting vector is continuous across the interface. Energy is transported by the ENZ medium, but not in a direction away from the interface. For  $p$  waves we find

$$\mathbf{S}(\mathbf{r})'_1 = 4\alpha\hat{\mathbf{k}}_{||}\sin^2(v_1\bar{z}), \quad (57)$$

$$\mathbf{S}(\mathbf{r})'_2 = 0. \quad (58)$$

The Poynting vector at the vacuum side is similar to that for  $s$  waves, but now we find that there is no energy flow at all in the material for  $p$  polarization. This is a direct consequence of the fact that the magnetic field in the medium is zero, as shown in Eq. (51).

## 7.2. Evanescent incident wave

For an evanescent incident wave,  $v_1$  is positive imaginary, and we have  $v_1^* = -v_1$ . We define

$$u = \sqrt{\alpha^2 - 1}, \quad (59)$$

so that  $v_1 = iu$  and  $u > 0$ . We now find for  $s$  waves

$$\mathbf{S}(\mathbf{r})'_1 = \alpha\hat{\mathbf{k}}_{||}[\exp(-u\bar{z}) + R_s(\alpha)^{ENZ}\exp(u\bar{z})]^2, \quad (60)$$

$$\mathbf{S}(\mathbf{r})'_2 = \alpha\hat{\mathbf{k}}_{||}[T_s(\alpha)^{ENZ}]^2\exp(-2\alpha\bar{z}). \quad (61)$$

For evanescent waves we have

$$R_s(\alpha)^{ENZ} = -(u - \alpha)^2, \quad (62)$$

$$T_s(\alpha)^{ENZ} = -2u(u - \alpha), \quad (63)$$

and both are real. It is easy to check that

$$[1 + R_s(\alpha)^{ENZ}]^2 = [T_s(\alpha)^{ENZ}]^2, \quad (64)$$

from which it follows that the Poynting vector is continuous across the interface. There is energy transport in the  $\mathbf{k}_{||}$  direction near the interface. For  $p$  waves we obtain

$$\mathbf{S}(\mathbf{r})'_1 = 4\alpha\hat{\mathbf{k}}_{||}\sinh^2(u\bar{z}), \quad (65)$$

$$\mathbf{S}(\mathbf{r})'_2 = 0. \quad (66)$$

We find again that for  $p$  waves no energy propagates through the material.

## 8. Normal incidence

Of practical importance is the case of normal or near normal incidence. In this case, the vector  $\mathbf{k}_{||}$  goes to zero, and  $\hat{\mathbf{k}}_{||}$  becomes undefined. We then assume a direction for  $s$  polarization chosen, and set

$$\hat{\mathbf{k}}_{||} = \mathbf{e}_s \times \mathbf{e}_z, \quad (67)$$

as follows from Eq. (11). For normal incidence we have  $\alpha = 0$ , and the expressions for the fields simplify considerably. The time dependent fields follow from the complex amplitudes as in Eq. (42).

With  $\nu_1 = 1$ ,  $R_s = 1$ ,  $\mathbf{e}_{p,i} = -\hat{\mathbf{k}}_{||}$ ,  $\mathbf{e}_{p,r} = \hat{\mathbf{k}}_{||}$  and  $T_s = 2$  we find for  $s$  polarization

$$\mathbf{E}(\mathbf{r}, t)_1 = 2E_0 \mathbf{e}_s \cos(\bar{z}) \cos(\omega t), \quad (68)$$

$$\mathbf{B}(\mathbf{r}, t)_1 = -2 \frac{E_0}{c} \hat{\mathbf{k}}_{||} \sin(\bar{z}) \sin(\omega t), \quad (69)$$

$$\mathbf{E}(\mathbf{r}, t)_2 = 2E_0 \mathbf{e}_s \cos(\omega t), \quad (70)$$

$$\mathbf{B}(\mathbf{r}, t)_2 = 0. \quad (71)$$

The electromagnetic field in vacuum is a standing wave, resulting from interference between the incident and reflected wave. The electric field in the ENZ material has no  $\mathbf{r}$  dependence. Its value is the same throughout the material, and it oscillates with angular frequency  $\omega$ . This is called ‘static optics’. The magnetic field is zero everywhere.

For  $p$  waves near normal incidence we obtain

$$\mathbf{E}(\mathbf{r}, t)_1 = -2E_0 \hat{\mathbf{k}}_{||} \cos(\bar{z}) \cos(\omega t), \quad (72)$$

$$\mathbf{B}(\mathbf{r}, t)_1 = -2 \frac{E_0}{c} \mathbf{e}_s \sin(\bar{z}) \sin(\omega t), \quad (73)$$

$$\mathbf{E}(\mathbf{r}, t)_2 = -2E_0 \begin{cases} \hat{\mathbf{k}}_{||} \cos(\omega t) & , \quad 0 \leq \alpha \ll |n| \\ \boldsymbol{\eta} \sin(\omega t) & , \quad |n| \ll \alpha \end{cases}, \quad (74)$$

$$\mathbf{B}(\mathbf{r}, t)_2 = 0. \quad (75)$$

The electric field in the ENZ material is again ‘static’. It is linearly polarized if  $\alpha$  is much closer to zero than  $|n|$ , and circularly polarized if  $|n|$  is much closer to zero than  $\alpha$ . When  $\alpha$  is seen as a variable, like in an angular spectrum, then there must be an abrupt, but smooth transition between the two polarization states.

Finally, we consider the time averaged Poynting vector in the limit of normal incidence. By considering the complex amplitudes in this limit, we find that in vacuum the value of  $\mathbf{E}(\mathbf{r}) \times \mathbf{B}(\mathbf{r})^*$  is imaginary, and therefore the Poynting vector vanishes. In the ENZ medium, the magnetic field is zero. Therefore, for normal incidence we have  $\mathbf{S}(\mathbf{r}) = 0$  everywhere.

## 9. Conclusions

We have studied the reflection off and the transmission through an ENZ interface. The incident field is taken as a plane wave, and we consider both traveling and evanescent incoming waves. The only variable in the problem is parameter  $\alpha$ . For a traveling incident wave ( $0 \leq \alpha < 1$ ) this is the sine of the angle of incidence, and for an evanescent incident wave ( $\alpha > 1$ ),  $1/\alpha$  is a dimensionless measure for the penetration depth. Moreover,  $k_o \alpha$  is the magnitude of the parallel components of all wave vectors (incident, reflected and transmitted).

First we have obtained the ENZ limit of the Fresnel reflection and transmission coefficients. We found that for  $p$  polarization of the incident wave the reflection coefficient is -1 for all  $\alpha$ . The

transmission coefficient vanishes for all  $\alpha$ , except for  $\alpha \ll |n|$  with both  $\alpha$  and  $n$  going to zero. Then the transmission coefficient is 2. Close to normal incidence ( $\alpha = 0$ ) there is an abrupt but smooth transition in the transmission coefficient for  $p$  waves. There is no such behavior for  $s$  polarized incident radiation. In that case, the absolute value of the reflection coefficient is unity for traveling incident waves and for  $\alpha > 1$  it drops to zero rapidly with increasing  $\alpha$ .

We then considered the electric and magnetic fields at both sides of the interface. At the vacuum side we have the usual interference between the incident and the reflected waves. In the ENZ medium all fields are evanescent for  $\alpha \neq 0$ . For an  $s$  polarized incident wave, the electric field in the ENZ medium is also  $s$  polarized. Remarkably, however, the magnetic field is exactly circularly polarized, and moves with a phase velocity of  $c/\alpha$  along the surface. For  $p$  polarized incident radiation, the magnetic field in the medium vanishes identically. The electric field is linearly polarized for  $0 \leq \alpha \ll |n|$  and circularly polarized for  $\alpha \gg |n|$ . For  $\alpha \gg |n|$ , the transmission coefficient is zero for all  $\alpha$ , but there is still an electric field. For normal incidence, the magnetic field in the medium is zero, both for  $s$  and  $p$  irradiation. The electric field is 'static', either linearly or circularly polarized. The Poynting vector in the medium for  $p$  waves is identically zero, but for  $s$  polarization there is a finite flow of energy along the surface.

## References

1. M. W. McCall, A. Lakhtakia, and W. S. Weiglhofer, "The negative index of refraction demystified," *Eur. J. Phys.* **23**(3), 353–359 (2002).
2. V. G. Vesalago, "The electrodynamics of substances with simultaneously negative values of  $\epsilon$  and  $\mu$ ," *Sov. Phys. Usp.* **10**(4), 509–514 (1968).
3. J. B. Pendry, "Negative refraction makes a perfect lens," *Phys. Rev. Lett.* **85**(18), 3966–3969 (2000).
4. X. Li and H. F. Arnoldus, "Fresnel coefficients for a layer of NIM," *Phys. Lett. A* **377**(34–36), 2235–2238 (2013).
5. B. Edwards, A. Alù, M. E. Young, M. G. Silveirinha, and N. Engheta, "Experimental verification of epsilon-near-zero metamaterial coupling and energy squeezing using a microwave waveguide," *Phys. Rev. Lett.* **100**(3), 033903 (2008).
6. H. Lobato-Morales, D. V. B. Murthy, A. Corona-Chávez, J. L. Olvera-Cervantes, and L. G. Guerrero-Ojeda, "Permittivity measurements at microwave frequencies using epsilon-near-zero (ENZ) tunnel structure," *IEEE Trans. Microw. Theory Tech.* **59**(7), 1863–1868 (2011).
7. V. Torres, B. Orzabayev, V. Pacheco-Peña, J. Teniente, M. Beruete, M. Navarro-Cía, M. S. Ayza, and N. Engheta, "Experimental demonstration of a millimeter-wave metallic ENZ lens based on the energy squeezing principle," *IEEE Trans. Antennas Propag.* **63**(1), 231–239 (2015).
8. M. Massaouti, A. A. Basharin, M. Kafesaki, M. F. Acosta, R. I. Merino, V. M. Orera, E. N. Economou, C. M. Soukoulis, and S. Tzortzakis, "Eutectic epsilon-near-zero metamaterial terahertz waveguides," *Opt. Lett.* **38**(7), 1140–1142 (2013).
9. V. Pacheco-Peña, N. Engheta, S. Kuznetsov, A. Gentshev, and M. Beruete, "Experimental realization of an epsilon-near-zero graded-index metalens at terahertz frequencies," *Phys. Rev. Appl.* **8**(3), 034036 (2017).
10. B. T. Schwartz and R. Piestun, "Total external reflection from metamaterials with ultralow refractive index," *J. Opt. Soc. Am. B* **20**(12), 2448–2453 (2003).
11. E. J. R. Vespeur, T. Coenen, H. Caglayan, N. Engheta, and A. Polman, "Experimental verification of  $n=0$  structures for visible light," *Phys. Rev. Lett.* **110**(1), 013902 (2013).
12. R. W. Ziolkowski, "Propagation in and scattering from a matched metamaterial having a zero index of refraction," *Phys. Rev. E* **70**(4), 046608 (2004).
13. A. Monti, F. Bilotti, A. Toscano, and L. Vegni, "Possible implementation of epsilon-near-zero metamaterials working at optical frequencies," *Opt. Commun.* **285**(16), 3412–3418 (2012).
14. S. Campione, D. de Ceglia, M. A. Vincenti, M. Scalora, and F. Capoloni, "Electric field enhancement in  $\epsilon$ -near-zero slabs under TM-polarized oblique incidence," *Phys. Rev. B* **87**(3), 035120 (2013).
15. A. A. Basharin, C. Mavdis, M. Kafesaki, E. N. Economou, and C. M. Soukoulis, "Epsilon near zero based phenomena in metamaterials," *Phys. Rev. B* **87**(15), 155130 (2013).
16. H. Iizuka and N. Engheta, "Antireflection structure for an effective refractive index near-zero medium in a two-dimensional photonic crystal," *Phys. Rev. B* **90**(11), 115412 (2014).
17. M. H. Javani and M. I. Stockman, "Real and imaginary properties of epsilon-near-zero materials," *Phys. Rev. Lett.* **117**(10), 107404 (2016).
18. M. Kamandi, C. Guclu, T. S. Luk, G. T. Wang, and F. Capoloni, "Giant field enhancement in longitudinal epsilon-near-zero films," *Phys. Rev. B* **95**(16), 161105 (2017).
19. M. G. Silveirinha and N. Engheta, "Tunneling of electromagnetic energy through subwavelength channels and bends using  $\epsilon$ -near-zero materials," *Phys. Rev. Lett.* **97**(15), 157403 (2006).
20. M. G. Silveirinha and N. Engheta, "Theory of supercoupling, squeezing wave energy, and field confinement in narrow channels and tight bends using  $\epsilon$ -near-zero metamaterials," *Phys. Rev. B* **76**(24), 245109 (2007).

21. A. Alù and N. Engheta, "Light squeezing through arbitrarily shaped plasmonic channels and sharp bends," *Phys. Rev. B* **78**(3), 035440 (2008).
22. D. A. Powell, A. Alù, B. Edwards, A. Vakil, Y. S. Kivshar, and N. Engheta, "Nonlinear control of tunneling through an epsilon-near-zero channel," *Phys. Rev. B* **79**(24), 245135 (2009).
23. B. Edwards, A. Alù, M. G. Silveirinha, and N. Engheta, "Reflectionless sharp bends and corners in waveguides using epsilon-near-zero effects," *J. Appl. Phys.* **105**(4), 044905 (2009).
24. A. Alù and N. Engheta, "Coaxial-to-waveguide matching with  $\epsilon$ -near-zero ultranarrow channels and bends," *IEEE Trans. Antennas Propag.* **58**(2), 328–339 (2010).
25. S. Enoch, G. Tayeb, P. Sabouroux, N. Guérin, and P. Vincent, "A metamaterial for directive emission," *Phys. Rev. Lett.* **89**(21), 213902 (2002).
26. A. Alù, M. G. Silveirinha, A. Salandrino, and N. Engheta, "Epsilon-near-zero-metamaterials and electromagnetic sources: tailoring the radiation phase pattern," *Phys. Rev. B* **75**(15), 155410 (2007).
27. B. Wang and K.-M. Huang, "Shaping the radiation pattern with mu and epsilon-near-zero metamaterials," *Prog. Electromagn. Res.* **106**, 107–119 (2010).
28. L. V. Alekseyev, E. E. Narimanov, T. Tumkur, H. Li, Y. A. Barnakov, and M. A. Noginov, "Uniaxial epsilon-near-zero metamaterial for angular filtering and polarization control," *Appl. Phys. Lett.* **97**(13), 131107 (2010).
29. F. J. Rodríguez-Fortuño, A. Vakil, and N. Engheta, "Electric levitation using  $\epsilon$ -near-zero metamaterials," *Phys. Rev. Lett.* **112**(3), 033902 (2014).
30. S. Feng and K. Halterman, "Coherent perfect absorption in epsilon-near-zero metamaterials," *Phys. Rev. B* **86**(16), 165103 (2012).
31. J. Yoon, M. Zhou, M. A. Badsha, T. Y. Kim, Y. C. Yun, and C. K. Hwangbo, "Broadband epsilon-near-zero perfect absorption in the near-infrared," *Sci. Rep.* **5**(1), 12788 (2015).
32. Z. Guo, F. Wu, C. Xue, H. Jiang, Y. Sun, Y. Li, and H. Chen, "Significant enhancement of magneto-optical effect in one-dimensional photonic crystals with a magnetized epsilon-near-zero defect," *J. Appl. Phys.* **124**(10), 103104 (2018).
33. H. F. Arnoldus and J. T. Foley, "Traveling and evanescent parts of the electromagnetic Green's tensor," *J. Opt. Soc. Am. A* **19**(8), 1701–1711 (2002).
34. H. F. Arnoldus, "Evanescent waves in the near- and the far field," in *Advances in Imaging and Electron Physics*, vol. **132**, P. W. Hawkes, ed. (Elsevier Academic Press, 2004), pp. 1–67.
35. L. Mandel and E. Wolf, *Optical Coherence and Quantum Optics*, Sec. 3.2.4 (Cambridge U. Press, 1995).
36. H. F. Arnoldus and J. T. Foley, "Transmission of dipole radiation through interfaces and the phenomenon of anti-critical angles," *J. Opt. Soc. Am. A* **21**(6), 1109–1117 (2004).
37. H. F. Arnoldus, M. J. Berg, and X. Li, "Transmission of electric dipole radiation through an interface," *Phys. Lett. A* **378**(9), 755–759 (2014).
38. H. F. Arnoldus and M. J. Berg, "Energy transport in the near field of an electric dipole near a layer of material," *J. Mod. Opt.* **62**(3), 218–228 (2015).